



HAL
open science

Quantum parameters for guiding the design of Ti-alloys with shape memory and/or low elastic modulus

Milena Arciniegas, Javier Peña, Jose Maria Manero, Juan Carlos Paniagua,
Javier Gil Mur

► **To cite this version:**

Milena Arciniegas, Javier Peña, Jose Maria Manero, Juan Carlos Paniagua, Javier Gil Mur. Quantum parameters for guiding the design of Ti-alloys with shape memory and/or low elastic modulus. Philosophical Magazine, 2008, 88 (17), pp.2529-2548. 10.1080/14786430802375667. hal-00513950

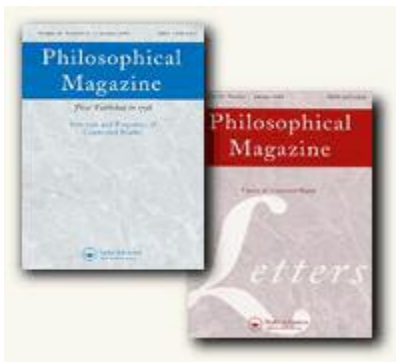
HAL Id: hal-00513950

<https://hal.science/hal-00513950>

Submitted on 1 Sep 2010

HAL is a multi-disciplinary open access archive for the deposit and dissemination of scientific research documents, whether they are published or not. The documents may come from teaching and research institutions in France or abroad, or from public or private research centers.

L'archive ouverte pluridisciplinaire **HAL**, est destinée au dépôt et à la diffusion de documents scientifiques de niveau recherche, publiés ou non, émanant des établissements d'enseignement et de recherche français ou étrangers, des laboratoires publics ou privés.



Quantum parameters for guiding the design of Ti-alloys with shape memory and/or low elastic modulus

| | |
|-------------------------------|--|
| Journal: | <i>Philosophical Magazine & Philosophical Magazine Letters</i> |
| Manuscript ID: | TPHM-08-Jul-0255 |
| Journal Selection: | Philosophical Magazine |
| Date Submitted by the Author: | 18-Jul-2008 |
| Complete List of Authors: | Arciniegas, Milena; Technical University of Catalonia, Department of Materials Science and Metallurgy Peña, Javier; Technical University of Catalonia, Department of Materials Science and Metallurgy; Escola Superior en Disseny ELISAVA, Department of Materials Science Manero, Jose Maria; Technical University of Catalonia, Department of Materials Science and Metallurgy Paniagua, Juan Carlos; University of Barcelona, Department of Physical Chemistry Gil Mur, Javier; Technical University of Catalonia, Department of Materials Science and Metallurgy |
| Keywords: | density-functional theory, shape memory alloys, titanium alloys |
| Keywords (user supplied): | low elastic modulus |
| | |



Quantum parameters for guiding the design of Ti-alloys with shape memory and/or low elastic modulus

M. Arciniegas^{1*}, J. Peña^{1,2}, J. M. Manero¹, J. C. Paniagua³ and F. J. Gil¹

^{1*}To whom correspondence should be addressed: Biomaterials and Biomechanics division, Department of Materials Science and Metallurgy, Technical University of Catalonia (UPC). Avda. Diagonal 647, Barcelona, 08028, Spain. Tel: +34-934-054-452, Fax: +34-934-016-706.

Email: milena.arciniegas@upc.edu.

²Department of Materials Science. Escola Superior en Disseny ELISAVA. C/Ample 11-13, 08002 Barcelona, Spain.

³Department of Physical Chemistry, University of Barcelona. Martí i Franqués 1, 08028. Barcelona, Spain.

Abstract

Electronic structure calculations based on density functional theory have been applied to clusters of titanium with different alloying elements in order to obtain quantum parameters that give some information on the interaction between the mother and alloying atoms. Average values of these parameters weighted with the molar fractions have been calculated for 146 titanium alloys that exhibit shape memory and/or low elastic modulus. These values have been mapped in order to identify zones that group the alloys with either property. This information has been used as a guide for designing seven new alloys with desired properties. These have been microstructurally and mechanically characterized, and the results confirm the usefulness of the method.

Keywords: titanium alloys, shape memory alloys, low elastic modulus, density functional theory.

1. Introduction

Since 1963, when the shape memory effect was discovered on Ti-Ni alloys, different properties have been studied on the basis of the reversible phase transformation austenite-martensite caused by temperature change or stress applied on the material [1-4]. These include superelasticity, simple and double shape memory effects, high damping and outstanding wear behaviour. Advantages from these interesting properties have been taken in biomedical applications, for example osteosynthesis plates, jaw plates, orthodontic archwires, stents and dental implants [5-7]. The shape memory together with the high corrosion resistance and excellent biocompatibility of Ti give a good fulfilment of the strict requirements of such applications [8-10]. Several studies have been published about mechanical and biological properties of TiNi and the relationship between them [1,8]. Some controversy exists on the risk of Ni ions release from the implant to the surrounding tissue, which can produce adverse reactions [11-13]. Two ways of overcoming this problem have been proposed: surface modification by means of surface coating oxidation [14,15] and substitution of Ni by biocompatible and non-citotoxics alloying elements that preserve the excellent shape memory properties of Ti-Ni alloys [16-18].

Another aspect frequently reported in the literature is the stress-shielding effect caused by mechanical non-compatibility between bone and implant; a too stiff material absorbs the load and hinders bone regeneration [7,11]. Different Ti alloys have been studied for reducing the elastic modulus of implant material so as to favour bone regeneration. The most common approach consists in using non-toxic β -stabilizing alloying elements, such as Ta, Nb, Mo, Hf and sometimes also Zr, because the β -phase Ti alloys show lower

1
2
3 elastic modulus compared to the α -phase ones [19-20]. In order to guide the design of
4 such alloys some researchers [21-23] have used a method based on molecular orbital
5 theory, which was introduced by Morinaga and co-workers in 1988 [24, 25]. The aim of
6 this method is to calculate quantum parameters that take into consideration the alloying
7 element effect for predicting the stable phase of Ti-alloys. The parameters chosen by
8 those authors the average bond order between the alloying and mother atoms and the
9 mean energy of virtual d -orbitals centred upon the alloying element. A recently published
10 article analyses the relationship of elastic properties with those parameters for a set of
11 twenty alloys [26].
12
13
14
15
16
17
18
19
20
21
22
23
24
25
26

27 With these precedents in mind, we have done a review of works published from 1970 up
28 to 2007, with the purpose of setting up a data base of Ti-alloys with low elastic modulus
29 and/or shape memory effect. This data base collects 146 alloys and includes their heat
30 and mechanical treatment, phase, elastic modulus and martensite start temperature (M_s
31 temperature). In an attempt of improving the theoretical method for designing Ti alloys
32 with the desired properties, a new set of parameters has been calculated by using a more
33 modern quantum methodology, based on the Density Functional Theory. The application
34 of the resulting parameters to the alloy data base has permitted to build a new map in
35 which zones can be delimited for the alloys with shape memory and/or low elastic
36 modulus. Although most of the alloys on the data base are biocompatible, some alloying
37 elements with controversial biocompatibility behaviour, such as Fe, Al, V or Ni –the
38 latter two under discussions [21] – have also been included for aiding to delimit the
39 zones.
40
41
42
43
44
45
46
47
48
49
50
51
52
53
54
55
56
57
58
59
60

The new map has been used as a guide to design seven new alloys with low elastic modulus and/or memory shape. These have been microstructurally and mechanically characterized for measuring the elastic modulus and verifying the presence of thermoelastic martensite phase transformation induced by temperature, but also by stress under indentation conditions. Phase transformations can be evidenced on the load vs. displacement into surface ($P-h$) curves as events on the loading and unloading portions, such as pop-in, pop-out or hysteresis loops produced between load and reload cycles [27]. These latter have been well reported by V. Domnich and G. Gogotsi in other transforming materials, such as silicon, gallium arsenide and zirconium oxide [28], by X.G. Ma *et al.* [29] in TiNi shape memory thin films and by C.P. Frick *et al.* [30] in nickel-titanium sub-micron compression pillars.

2. Map generation

2.1 Calculation of the new parameter set

The parameters proposed by Morinaga and co-workers for charting the alloys are averages of the bond order between the alloying and mother elements (Bo) and of the mean energy of the lowest virtual d -orbitals of symmetry t_{2g} and e_g centred upon the alloying element (Md). These averages are weighted with the atomic fraction of each alloying element (x_i) [24]:

$$\overline{Bo} = \sum_{i=1}^{i=n} x_i \cdot Bo_i \quad (\text{Eqn. 1})$$

$$\overline{Md} = \sum_{i=1}^{i=n} x_i \cdot Md_i \quad (\text{Eqn. 2})$$

1
2
3 where n is the number of alloying elements in the alloy.
4

5
6 A cluster of 14 mother atoms surrounding one alloying atom with bcc structure was
7
8 adopted for calculating the values of Bo_i and Md_i for each alloying element, and the
9
10 Discret Variational $X\alpha$ (DV- $X\alpha$) method was used as computational tool [31]. It is
11
12 assumed that Bo_i provides some measure of the strength of the bond between the alloying
13
14 and mother elements, and Md_i correlates with the electronegativity and metallic radius of
15
16 the alloying atom.
17
18

19
20 In the present work a new set of parameters has been calculated by using the Khon-Sham
21
22 implementation of Density Functional Theory (DFT) with the hybrid exchange-
23
24 correlation functional B3LYP [32,33]. DFT electronic structure calculations have proven
25
26 a great success in obtaining properties of molecules and solids, and it is now well
27
28 established as a useful tool for research in material science [34]. Over other electronic
29
30 structure calculation methods of comparable accuracy it has the advantage of being
31
32 conceptually simpler and very efficient from the computational point of view. The effect
33
34 of internal electrons has been taken into account by means of the effective core potentials
35
36 proposed by Hay and Wadt [35-37], that include some relativistic effects. The basis set
37
38 used is the split-valence one put forward by Dunning *et al.* [38]. All the calculations have
39
40 been done with the Gaussian package [39].
41
42
43
44
45
46
47

48
49 As in Morinagas's approach, a cluster of 14 mother atoms surrounding one alloying atom
50
51 with bcc structure has been adopted to model the alloy. Cluster models have been used to
52
53 model a wide variety of bulk properties of solids atoms [40], and they are considered a
54
55 complement to band theory especially useful for studying local properties, as is the case
56
57
58
59
60

1
2
3
4 for the interaction of an alloying atom with the surrounding mother. Although the
5
6 calculation results are dependent on the geometry of the cluster, the resulting differences
7
8 can be overlooked, given the crude character of the parameters to be obtained [24]. While
9
10 Morinaga used the energy of virtual d -orbitals to obtain one of the parameters, we have
11
12 referred to referred it to the energy of occupied orbitals centered upon the alloying
13
14 element. These are more localized and more basis set independent than the virtual ones,
15
16 which usually have energies rather dependent on the basis set choice. On the other hand,
17
18 their changed-sign energies provide good approximations to the corresponding ionization
19
20 potentials [41,42]. These, in turn, are related to the Mulliken electronegativity, which is
21
22 defined as the mean of the ionization potential and the electron affinity of the system.
23
24 For each cluster we have carefully investigated different orbital occupations and spin
25
26 multiplicities in order to find the ground electronic state. Then we have selected the
27
28 highest occupied molecular orbital centered upon the alloying atom (HOMOAL), its
29
30 absolute-value energy (OE) being a measure of the ionization potential of that atom in the
31
32 cluster. The bond orders between the alloy and mother elements (BO) have been
33
34 calculated by a natural poblational analysis (atom-atom overlap-weighted natural atomic
35
36 orbital bond order, see [43]). This definition produces bond orders that are little
37
38 dependent on the basis set choice, if minimal bases are not taken in account [44-45].
39
40
41
42
43
44
45
46
47

48 The BO and OE parameters obtained for the elements of the studied alloys are listed in
49
50 Table 1, together with the values previously obtained by Morinaga and co-workers. It
51
52 should be pointed out that OE values are expressed in atomic energy unities (hartrees),
53
54 while Md values are reported in electron-volts. To obtain the weighted average values of
55
56
57
58
59
60

1
2
3 these parameters for each alloy expressions analogous to equations (1) and (2) have been
4 used. The data of table 1 disclose that Md values calculated by Morinaga and the OE
5 values calculated in the present work do not have a parallel behaviour. As already stated,
6
7
8
9
10 Morinaga orbital energies are obtained from virtual orbitals obtained with DV- $X\alpha$ type
11
12
13 calculations. These bear some inverse relationship to electron affinities: the more positive
14
15 the energy the lower the electron affinity. On the other hand, our OE parameters are
16
17 occupied orbital energies resulting from DFT-B3LYT calculations that include
18
19 relativistic corrections, with the sign inverted in order to obtain positive numbers. Larger
20
21 values of this parameter correlate with larger ionization potentials. Since both, the
22
23 electron affinity and the ionization potential, contribute to Mulliken electronegativity one
24
25 could expect an inverse relationship between Md and BO ; however, Md is based on d
26
27 orbitals while OE refers to the HOMOAL, which have different degrees of s , p or d
28
29 character depending on the system. Therefore, no direct connection exists between both
30
31 parameters.
32
33
34
35
36
37
38

39 2.2 Ti-alloy data compilation

40
41 Table 2 collects 139 Ti-alloys reported on literature from 1970 to 2007 together with
42
43 seven alloys fabricated in our laboratory, completing a total of 146. All of the compiled
44
45 alloys present shape memory and/or are low elastic modulus according to the criterion of
46
47 their respective authors. Other significant data, such as the publication year, the heat
48
49 and/or mechanical treatments, the resulting phase, and the chemical composition, are also
50
51 included in the table. After a peak in 1994, the publication rhythm is, in the average,
52
53 approximately steady (see Fig.1). In some alloys with high β -stabilizing element content
54
55
56
57
58
59
60

1
2
3 some proportion of ω -phase is observed, as happens to those with numbers 1, 68-72, 113-
4
5
6 117. The ω -phase may be suppressed by addition of some α -stabilizer, as Al (see the
7
8 alloys 51a and 88), as well as by changing the heat treatment conditions (see the alloys
9
10 51b). Since the treatment influences the mechanical properties of the resulting material,
11
12 some alloys have more than one entry in the table, these being distinguished by adding a
13
14 letter to the alloy number (see, among others, the alloys numbered as 51-55 and 90). In a
15
16 few instances duplicity of data comes from different references reporting on the same
17
18 alloy.
19
20
21

22
23
24
25 The usual criterion for an alloy to be considered of low elastic modulus (LEM) has
26
27 changed somewhat along the time: until the nineties elastic modulus values under
28
29 125 GPa were usually considered low, while this threshold has lowered to about 90 in the
30
31 last years. Around 50% of the compiled alloys have an elastic modulus lower than this
32
33 latter value. β -phase alloys have, in general, lower elastic modulus than the α -phase ones,
34
35 which explains the high proportion of alloys with β -phase appearing in the table. Some
36
37 heat treatments –such as annealing and aging– tend to increase the elastic modulus, thus
38
39 explaining that of some of the β -phase alloys have relatively high values of that
40
41 parameter. This is the case of the alloys 33b (102 GPa), 35 (112 GPa) and 52b (113 GPa).
42
43 On the other hand, if the cooling rate is increased –using, for example, quench treatments
44
45 in ice-water– the β -phase is favoured and the elastic modulus is significantly reduced.
46
47 This reduction is particularly noticeable for some cold worked alloys such as 54a
48
49 (50 GPa) and 90d (44 GPa).
50
51
52
53
54
55
56
57
58
59
60

1
2
3 About one third of the alloys display shape memory effect (SME); however, this
4 proportion is not very meaningful, because many of the references do not mention this
5 aspect. Shape memory is usually reported by the presence of thermoelastic martensitic
6 plates induced by stress, but some of the articles only mention the martensite start
7 temperature (M_s).
8
9

10
11 A relevant number of the compiled alloys have been developed for being used in the
12 biomedical field. Low elastic modulus is a frequent requisite in this field; which explains
13 that the most common alloying elements are the highly biocompatible
14 β -stabilizers Ta, Nb and Mo [9]. Shape memory is also a desired property for some
15 biomedical applications such as cardiovascular stents, orthodontic wires and orthopedic
16 plates. The fact that some alloys exhibit both properties (see, for instance, 55, 56, 88, 110,
17 130 and 134) opens interesting possibilities not yet fully exploited such as their service in
18 load-transfer devices.
19
20
21
22
23
24
25
26
27
28
29
30
31
32
33
34
35

36 2.3. Alloy charts

37
38 The calculated BO and OE parameters (Table 1) have been used together with the
39 chemical compositions listed in the Table 2 to obtain, for each alloy, average values,
40 \overline{BO} and \overline{OE} , weighted with the molar fractions. These have been plotted in a two-
41 dimensional graph with different symbols for indicating the phase and the LEM and/or
42 SME properties (Fig. 2). The α and β phases are identified by a black star and a grey
43 circle, respectively, while a grey triangle indicates the coexistence of both phases.
44 Although a few alloys show a small proportion of a third ω -phase, these have been
45 identified according to the predominant phase. A hollow symbol indicates LEM, and a
46
47
48
49
50
51
52
53
54
55
56
57
58
59
60

1
2
3 multiplication sign is used for SME. These two symbols are superimposed when both
4 properties are present. For an alloy to be considered of low elastic modulus we have
5 adopted the more restrictive criterion based on a 90 GPa threshold. The equiatomic TiNi
6 alloy (number 56), which presents \overline{BO} and \overline{OE} values very different from those of the rest
7 of the alloys, has not been included in the diagram, so as to get a better differentiation of
8 the other points.
9

10
11
12
13
14
15
16
17
18
19
20 The α phase alloys appear at the right side of the map, while β alloys are mostly on the
21 left hand side. Those in which both phases coexist extent from the middle to the right
22 side. In fact, the presence of both phases indicates that the heat-mechanical treatment has
23 not lead to a complete transformation to the more stable phase. We have drawn a solid
24 line and a dotted one that enclose the alloys with LEM and those with SME, respectively.
25
26
27
28
29
30
31
32
33
34
35
36
37
38
39
40
41
42
43
44
45
46
47
48
49
50
51
52
53
54
55
56
57
58
59
60
The zones corresponding to these two properties are mostly on the left side of the map.
This agrees with the fact that α stabilizers tend to increase the elastic modulus. LEM
predominate in the upper part and SME in the lower side. Both zones overlap in a region
including the alloys for with both properties have been reported.

It should be noted that the drawn lines do not represent sharp frontiers, since each region
includes some alloys not bearing the corresponding property. This is due, on the one
hand, to the fact that the calculated parameters only provide a crude representation of the
structural features determining LEM and SME, and, on the other, to the mechanical
properties depending on the heat treatment applied to the alloy, which cannot be taken
into account in such a kind of maps. One should also take into consideration that in many

1
2
3 of the compiled works only one of those two properties has been studied, so that there
4 surely are more alloys with one or the other property than indicated. Thus, the drawn
5 frontiers are rather speculative, and should be reconsidered in the light of future
6 experimental information. Nevertheless, they provide valuable information on where to
7 look for alloys with desired properties, as we will later show.
8
9

10
11 For the sake of comparison we have also used Morinaga's parametrization to calculate
12 the *Bo* and *Md* values of the alloys collected in table 2, except for those containing the
13 elements oxygen (alloy 67) and gallium (alloys 92 and 93), which were not included in
14 the published list of parameters. The results have been plotted in Fig. 3 using the same
15 symbols as in Fig. 2, and zones enclosing the alloys with LEM and SME have been
16 delimited with the same criterion as in that figure. The first thing to note is that both maps
17 have a very different aspect, which is due to the arguments already mentioned while
18 discussing the data of Table 1: different quantum calculation method, bond order
19 definition and type of chosen orbital, and inclusion of relativistic corrections in the
20 pseudopotentials used for the present calculations, which can be relevant for atoms with
21 high atomic number. This is the case of some alloying elements that are particularly
22 useful for biomedical applications: Nb, Ta, Zr and Hf. In Fig. 3 most of the LEM zone is
23 included into the SME region, and the alloys with one or the other property appear rather
24 mixed, especially in the upper part of the diagram. In fact, Morinaga's parametrization
25 was not initially intended to represent those properties, but rather to differentiate phases
26 and deformation mechanisms (slip and twin), as well as to identify alloys that lead to
27 martensite on quenching. The zones corresponding to LEM and SME are more separated
28
29
30
31
32
33
34
35
36
37
38
39
40
41
42
43
44
45
46
47
48
49
50
51
52
53
54
55
56
57
58
59
60

1
2
3 in the map of Fig. 2, and they overlap in a smaller region with a high proportion of alloys
4 bearing both properties.
5
6
7
8
9

10 **3. Design of seven new alloys**

11 Many alloys with excellent mechanical properties for biomedical applications contain Ni
12 in their composition (see, for instance, the Ti-Ni-Cu-Mo alloys with numbers 84 to 87
13 and the Ti-Ni-Ta ones numbered 124, 125 and 126). However, the fact that the atoms of
14 this element released from an implant can produce adverse reactions has motivated the
15 search of new, Ni-free formulas for substituting those alloys. The above presented map
16 has been used to guide the design of seven new alloys, which are expected to show low
17 elastic modulus and/or shape memory. They are numbered consecutively from 128 to 134
18 in table 2, and their \overline{OE} and \overline{BO} coordinates are (0.1526, 0.6089) for the alloy numbered
19 128, (0.1530, 0.6079) for 129, (0.1540, 0.6054) for 130, (0.1524, 0.6101) for 131,
20 (0.1535, 0.6119) for 132, (0.1542, 0.6107) for 133 and (0.1533, 0.6070) for 134. The one
21 numbered 131 is clearly located in the LEM zone, at the left side of the map. Those with
22 numbers 128, 130, 132 and 133 are situated in the LEM zone near the boundary of the
23 SME region, and the measurement of their properties has permitted to better define that
24 boundary. The two remaining alloys (129 and 134) were chosen well inside the overlap
25 area.
26
27
28
29
30
31
32
33
34
35
36
37
38
39
40
41
42
43
44
45
46
47
48
49
50

51 3.1. Experimental procedure

52 The alloys were fabricated using an electric arc furnace in controlled Ar atmosphere, cast
53 in 40 g buttons from bars of the starting elements of 99.9% purity. The buttons were
54
55
56
57
58
59
60

1
2
3 melted five times for enhancing the material homogenization and avoiding segregation of
4 the heavier elements. Then, buttons were encapsulated within a vacuum quartz tube,
5
6 solution treated at 1100°C for 1.5 hours and quenched in ice-water. Samples of both
7
8 alloys were mounted on Bakelite, mechanically polished and finished with colloidal silica
9
10 to give a average surface roughness of <100nm for using in the different characterization
11
12 techniques. A Fischerscope X-ray System HDL equipment was used for verifying the
13
14 chemical composition. The tests were conducted on four different positions –from centre
15
16 to periphery– of each sample for evaluating the chemical homogeneity. The samples were
17
18 etched with Keller reactive (2 ml HF, 3ml HCl, 5 ml HNO₃ and 190 ml H₂O) for optical
19
20 microstructural analysis. A differential scanning calorimeter (DSC) Q1000 TA
21
22 Instrument was used for determining the presence of thermoelastic phase transformation
23
24 and its corresponding temperatures. With the purpose to remove the thermal and
25
26 mechanical history on the alloys, which could modify the phase transformation
27
28 temperatures, 2 cycles of heating and cooling were applied from -90°C to 200°C. Then,
29
30 only the second cycle was used for determining the transformation temperatures by
31
32 means of the line intercept method. Rectangular plates of 10 x 10 x 25 mm were
33
34 machined, ground, and polished after heat treatment for measuring the elastic modulus by
35
36 ultrasounds transmission method at room temperature using a USN50 ultrasound
37
38 instrument. The tests were conducted by means of transmitters of longitudinal and
39
40 transversal waves, which were coupled on the specimen surface. A coupling-solution was
41
42 employed in order to improve the wave propagation. The elastic modulus was calculated
43
44 by means of the Eqn. 3 and 4.
45
46
47
48
49
50
51
52
53
54
55
56
57
58
59
60

$$\nu = 1 - \frac{1}{2} \cdot \frac{1}{1 - \left(\frac{C_t}{C_l}\right)^2} \quad (\text{Eqn. 3})$$

$$E = 2 \cdot \rho \cdot (1 + \nu) \cdot C_t^2 \quad (\text{Eqn. 4})$$

where C_t and C_l are the transversal and longitudinal wave velocities, respectively, ν is the Poisson coefficient and ρ is the alloy density. The error was 5% approximately, estimated from the error in specimen dimension generated by polishing.

Finally, on each sample of the studied alloys fifteen cyclic instrumented indentation tests were performed, in which the load was linearly increased up to the maximum of 625 mN, using an MTS System Nano Indenter XP. The tests were carried out using a spherical tip with a radius of 750 nm in order to evaluate the phase transformation induced by stress in the new alloys under indentation loading. All tests were conducted at room temperature and started when the thermal drift was maintained lower than 0.05 nms^{-1} . The thermal drift was estimated and corrected during the test automatically. A strain rate of 0.05 s^{-1} was applied in loading, unloading and reloading. In order to guarantee the contact throughout the test, the indenter was unloaded after every cycle up to 95% of the maximum load applied in the cycle.

3.2 Microstructure, physics and mechanical properties of the new alloys

The relevant properties of the seven new alloys are collected in Table 3. Only a wt % variation of alloying element lower to 1% was estimated between the theoretical chemical composition and those determined by x-ray fluorescence. No significant differences were

1
2
3 found between centre and periphery of the samples, which indicates a good
4
5 homogenization of the studied alloys in the established composition.
6
7

8
9
10
11 Fig. 4 shows representative optical micrographs for the different microstructures of the
12 studied alloys: β -prior grains homogenously distributed on the samples of the new alloys
13 numbered as 128, 131 and 132 (see Fig. 4a from the alloy numbered as 131), β -prior
14 grains accompanied by acicular and short plates on the alloys numbered as 129 and 133
15 (see Fig. 4b from the alloy numbered as 129), and acicular and fine plates of different
16 sizes within β -prior grains on the alloys numbered 130 and 134 (see Fig. 4c from the
17 alloy numbered as 134). X-ray diffraction profiles of the new alloys, shown in Fig. 5,
18 confirmed the presence of the β -phase, especially in the alloys numbered as 128, 131 and
19 132, associated to the (002), (200) and (211) diffraction planes. Also, the α'' -phase was
20 detected in the rest of the new alloys, particularly in the alloys numbered as 130 and 134,
21 in which a characteristic double pick of this phase, around 40° of theta angle, was
22 observed on the x-ray profiles. These results are in agreement with the predictions from
23 the maps (see Fig. 2) and confirm the relation between β -stabilizer content and amount of
24 α'' -martensite plates: an increment of β -stabilizer content decreases the α'' -phase fraction
25 by hindering the α'' plates nucleation [70].
26
27
28
29
30
31
32
33
34
35
36
37
38
39
40
41
42
43
44
45
46
47
48
49
50

51 In order to evidence the temperature-induced thermoelastic martensitic phase
52 transformation that can taken place, the new alloys were analysed by DSC. Reversible
53 changes of thermodynamic baseline associated to the one-step reversible phase
54
55
56
57
58
59
60

1
2
3 transformation from austenite to martensite on heating and cooling [1-3], with an M_s
4 temperatures of 125°C and 45°C, for the Ti-13.7Nb-1.4Ta (130) and Ti-19.1Nb-8.8Zr
5 (134) alloys, respectively, were appreciated on the DSC profiles, whereas the rest of the
6 alloys did not evidence any martensitic transformation (see Fig. 6 in which the DSC plot
7 obtained from the alloy 134 in contrast with that obtained from the alloy 131 are shown).
8 Contrarily to what was expected by the authors, the new alloys numbered as 129 and 130
9 did not present temperature induced reversible phase transformation, although they were
10 designed inside of the SME zone (see Fig. 2) and presented α'' -thermoelastic martensite
11 phase, detected by x-ray diffraction. This can be explained by a low fraction of α'' -phase,
12 which restrains the transformation capability or a transformation temperature out of the
13 testing conditions.
14
15
16
17
18
19
20
21
22
23
24
25
26
27
28
29
30
31

32 According with the results of the ultrasound tests, the alloys object of this study show
33 elastic moduli values in a range from 67 to 79 GPa. As predicted by the design method,
34 all values are relatively low compared with alloys currently employed in the biomedical
35 field.
36
37
38
39
40
41
42
43

44 Finally, with the purpose to evidence the stress-induced thermoelastic martensitic phase
45 transformation (TPT) the new alloys were subjected to indentation tests. Thin and well
46 defined hysteresis loops produced between load and reload cycles were observed in all
47 the P-h curves obtained from the alloys numbered as 128, 129, 130 and 134 (see Fig. 6 in
48 which one representative P-h curve of the alloys numbered as 128 is shown in solid line),
49 whereas the rest of the alloys no changes in the P-h curves were appreciated (see Fig. 6 in
50
51
52
53
54
55
56
57
58
59
60

1
2
3 which one representative P-h curve of the alloys numbered as 132 is shown in dashed
4 line). Such difference between the unloading and reloading path is explained by the fact
5 that in transforming materials, when load is released, both the elastic response (prevalent
6 in the beginning) and the phase transformation in the form of continuous reverse
7 twinning (when the stress decreases below the critical stress for transformation)
8 contribute to the recovery, and during the successive reloading a different stress state
9 activates again the transformation, which generates the observed loops. Similar behaviour
10 have been reported in other type of transforming materials [71] and by C.P Frick *et al.*
11 [30,72] on TiNi alloys at very low indentation depth and also evidenced under cyclic
12 uniaxial tests of shape memory alloys [73,74]. Conversely, in cyclic loading of non-
13 transforming materials, the unloading portion of a *P-h* curve is completely elastic and the
14 subsequent reloading follows the same path. In order to confirm that such differences
15 between unloading and reloading path are due to the presence of induced-stress phase
16 transformation, the P-h curves obtained were analyzed using the power law relation
17 proposed by W.C. Oliver *et al.* [75], which shows that during elastic unloading and
18 reloading, the relation between load (P) and displacement into surface (h) is given by:

$$P \propto (h - h_f)^{1.5} \quad (\text{Eqn. 5})$$

19 Accordingly, the material is reloaded elastically until the maximum load of the previous
20 cycle is reached, thereafter plastic deformation is resumed. In our transforming materials,
21 strong deviation from such relation was manifested, confirming that the response is due
22 not only to elastic recovery, but also to phase transformation. Non-transforming
23 materials, conversely, showed good agreement with the mentioned law.
24
25
26
27
28
29
30
31
32
33
34
35
36
37
38
39
40
41
42
43
44
45
46
47
48
49
50
51
52
53
54
55
56
57
58
59
60

1
2
3
4
5
6 The alloys 128, 129, 130 and 134 are especially interesting because they combine a rather
7
8 low elastic modulus with shape memory effect; in particular, the latter two, that exhibit a
9
10 change of phase activated by temperature variation. The transformation temperature
11
12 could be modified through mechanical and/or heat treatment so as to conform to the
13
14 needs of certain biomedical applications.
15
16

17 18 19 20 **4. Conclusions**

21
22 Theoretical parameters have been calculated by applying density functional theory to
23
24 clusters of 14 titanium atoms surrounding different alloying central elements in order to
25
26 model the interaction between Ti and the alloying atom. A compilation of data on 146 Ti-
27
28 alloys with shape memory and/or low elastic modulus has permitted to characterize each
29
30 alloy with averages of those parameters weighted with the molar fraction of its
31
32 components, and these data have been used to draw a map where regions corresponding
33
34 to those two properties can be delimited. This map has been used as a guide for searching
35
36 new alloys with good qualities for medical use. Seven new alloys have been designed and
37
38 microstructurally and mechanically characterized. As expected from the map, all of
39
40 them present low elastic modulus, and some of them also have memory shape, which has
41
42 been used for better defining the boundary of the corresponding zone. Two of them
43
44 present martensite phase transformation thermally induced with M_s temperatures of
45
46 125°C and 45°C respectively, which could be modified through mechanical and/or heat
47
48 treatment for applications that require a transformation at body temperature. Other two
49
50 alloys show stress-induced phase transformation under cyclic nanoindentation conditions.
51
52
53
54
55
56
57
58
59
60

1
2
3 These results confirm the usefulness of the proposed methodology for guiding the search
4
5 of alloys with LEM and/or SME.
6
7

10 **Acknowledgements**

11
12 The authors wish to thank Spanish Ministry of Science and Technology for financial
13
14 support through grants MAT2005-07244-C03-01, CTQ2005-08459-CO2-01 and
15
16 BIO2004-05436. They also want to acknowledge the referees for useful comments.
17
18
19

22 **References**

- 23
24 [1] T.W. Duering, A.R. Pelton. Ti-Ni Shape Memory Alloys. In: R. Boyer, G. Welsch,
25
26 E.W. Collings, editors. *Materials Properties Handbook Titanium Alloys*, ASM
27
28 International, 1994. p.1035.
29
30
31 [2] T.W. Duering, K.N. Melton, C.M. Wayman. *Engineering aspects of shape memory*
32
33 *alloys*. Ed. Butterworth-Heinemann Ltd., 1990.p.3
34
35
36 [3] B.G. Mellor. Martensitic transformation and the shape memory effect. In: *Science*
37
38 *and technology of shape memory alloys*. Ed. V. Torra, 1987, p.274.
39
40
41 [4] E. Hornbogen: *Prakt. Metallogr.* (Germany), 1989, vol. 26, p. 279.
42
43
44 [5] K. Wang. *Mater. Sci. Eng. A*, 213, 1996, 134-137.
45
46
47 [6] M. Long, H.J. Rack. *Biomaterials*, 19, 1998, 1621-1639.
48
49
50 [7] M. Niinomi. *Sci. Technol. Adv. Mater.*, 4, 2003, 445-454.
51
52
53 [8] S.G. Steinemann. *Surface performance of Titanium*. Warrendale, PA:TMS33-45,
54
55 1996.
56
57 [9] Y.Okazaki, Y. Ito, K. Kyo, T. Tateisi. *Mater. Sci. Eng. A*213, 1996, 138-147.
58
59
60

- 1
2
3
4
5
6
7
8
9
10
11
12
13
14
15
16
17
18
19
20
21
22
23
24
25
26
27
28
29
30
31
32
33
34
35
36
37
38
39
40
41
42
43
44
45
46
47
48
49
50
51
52
53
54
55
56
57
58
59
60
- [10] S.A. Shabalovskaya. *Intern. Mat. Review.* 46, 2001, 233-250.
- [11] M. Niinomi. *Metall. Mater. Trans. A*, 32, 2001, 477-486.
- [12] M. Niinomi. *JOM.*, 51, 1999, 32-34.
- [13] K. Wang. *Mater. Sci. Eng. A*, 213, 1996, 134-137.
- [14] A. Michiardi, C. Aparicio, J.A. Planell, F.J. Gil. *J. Biomed. Mater. Res. Part B: Appl Biomater.*, 77B, 2006, 249-256.
- [15] S.A. Shabalovskaya. *Bio-med. Mat. Eng.* 6, 1996, 267-289.
- [16] Y. Fukui, T. Inamura, H. Hosoda, K. Wakashima, S. Miyasaki. *Mater. Trans.*, 45, 2004, 1077-1082.
- [17] J.-P. Noh, D.-W. Chung, H.-W. Lee, T.-H. Nam. *Mater. Sci. Technol.*, 17, 2001, 1544-1550.
- [18] T. Grosdidier, M. J.Philippe. *Mater. Sci. Eng. A.*, 291, 2000, 218-223.
- [19] Y. Okasaki. *Curr. Opin. Solid State Mater. Sci.*, 5, 2001, 45-53.
- [20] Y.H. Hon, J.Y. Wang, Y.N. Pan. *Mater. Lett.*, 58, 2004, 3182-3186.
- [21] D. Kuroda, M. Niinomi, M. Morinaga, Y. Kato, T. Yashiro. *Mater. Sci. Eng.* 243, 1998, 244-249.
- [22] M. Morinaga, M. Yoshinori, Y. Hisoshi. *Mater. Sci. For.*, 449, 2004, 37-42.
- [23] Saito T. et.al. *Science*, 300, 2003, 464-467.
- [24] M. Morinaga, M. Kato, T. Kamimura, M. Fukumoto, I. Harada, K. Kubo. In: *Sixth World Conference on Titanium*. Francia, vol. 1, 1988, p. 1601.
- [25] M. Morinaga, N. Yukawa. In: *Computer Aided Innovation of New Materials*. Japon, 1991, p. 803.
- [26] H. Adachi, M. Tsukada, C. Sakoto. *J. Phys. Soc. Japan* 45, 1978, 875-883.

- 1
2
3 [27] M. Arciniegas, J.M. Manero, J. Peña, F.J. Gil, J.A. Planell. *Met. Mater. Trans. A*,
4 39, 2008, 742-751.
5
6
7
8 [28] V. Domnich, Y. Gogotsi. Phase transformation in silicon under contact loading.
9 *Rev. Adv. Mater. Scie.*, 3, 2002, 1-36.
10
11
12 [29] X.G. Ma, K. Komvopoulos. In situ transmission electron microscopy and
13 nanoindentation studies of phase transformation and pseudoelasticity of shape-memory
14 titanium-nickel films. *J. Mater. Res.*, 20, 2005, 1808-1813.
15
16
17
18 [30] C.P. Frick, S. Orso, E. Arzt. Loss of pseudoelasticity in nickel–titanium sub-
19 micron compression pillars. *Acta Mater.*, 55, 2007, 3845-3855.
20
21
22 [31] M. Abdel-Hady, K. Hinoshita, M. Morinaga. *Scripta Mater.* 55, 2006, 477-480.
23
24
25 [32] A. D. Becke. *J. Chem. Phys.* 98, 1993, 5648.
26
27
28 [33] C. Lee, W. Yang, R. G. Parr. *Phys. Rev. B* 37, 1988, 785.
29
30
31 [34] W. Koch, M. C. Holthausen. *A Chemist's Guide to Density Functional Theory*,
32 2nd ed., Wiley-VHC, Weinheim, 2001.
33
34
35 [35] P. J. Hay, W. R. Wadt. *J. Chem. Phys.* 82, 1985, 270.
36
37
38 [36] W. R. Wadt, P. J. Hay. *J. Chem. Phys.* 82, 1985, 284
39
40
41 [37] W. R. Wadt, P. J. Hay, *J. Chem. Phys.* 82, 1985, 299.
42
43
44 [38] T. H. Dunning Jr. and P. Hay. In: *Modern Theoretical Chemistry*. Ed. H. F.
45 Schaefer III, 3, 1. New York, 1976.
46
47
48 [39] Gaussian 03, Revision C.02, M. J. Frisch, G. W. Trucks, H. B. Schlegel, G. E.
49 Scuseria, M. A. Robb, J. R. Cheeseman, J. A. Montgomery, Jr., T. Vreven, K. N.
50 Kudin, J. C. Burant, J. M. Millam, S. S. Iyengar, J. Tomasi, V. Barone, B. Mennucci, M.
51 Cossi, G. Scalmani, N. Rega, G. A. Petersson, H. Nakatsuji, M. Hada, M. Ehara, K.
52
53
54
55
56
57
58
59
60

- 1
2
3
4
5
6
7
8
9
10
11
12
13
14
15
16
17
18
19
20
21
22
23
24
25
26
27
28
29
30
31
32
33
34
35
36
37
38
39
40
41
42
43
44
45
46
47
48
49
50
51
52
53
54
55
56
57
58
59
60
- Toyota, R. Fukuda, J. Hasegawa, M. Ishida, T. Nakajima, Y. Honda, O. Kitao, H. Nakai,
M. Klene, X. Li, J. E. Knox, H. P. Hratchian, J. B. Cross, C. Adamo, J. Jaramillo, R.
Gomperts, R. E. Stratmann, O. Yazyev, A. J. Austin, R. Cammi, C. Pomelli, J. W.
Ochterski, P. Y. Ayala, K. Morokuma, G. A. Voth, P. Salvador, J. J. Dannenberg, V. G.
Zakrzewski, S. Dapprich, A. D. Daniels, M. C. Strain, O. Farkas, D. K. Malick, A. D.
Rabuck, K. Raghavachari, J. B. Foresman, J. V. Ortiz, Q. Cui, A. G. Baboul, S. Clifford,
J. Cioslowski, B. B. Stefanov, G. Liu, A. Liashenko, P. Piskorz, I. Komaromi, R. L.
Martin, D. J. Fox, T. Keith, M. A. Al-Laham, C. Y. Peng, A. Nanayakkara, M.
Challacombe, P. M. W. Gill, B. Johnson, W. Chen, M. W. Wong, C. Gonzalez, and J. A.
Pople, Gaussian, Inc., Wallingford CT, 2004.
- [40] G. Pacchioni, P. S. Bagus and F. Parmigiani, Cluster Models for Surface and Bulk
Phenomena, NATO ASI Series, Series B: Physics Vol. 283, Plenum Press, New York,
1992.
- [41] D. P. Chong, O. V. Gritsenko, E. J. Baerends, J. of Chem. Phys. 116, 1760-1772,
2002.
- [42] S. Hamel, P. Duffy, M. E. Casida, D. R. Salahub, J. Electron Spectrosc. Relat.
Phenom. 123, 345-363, 2002.
- [43] J. E. Carpenter, F. Weinhold, J. Mol. Struct. (Theochem.) 169, 41, 1988.
- [44] A. E. Reed, F. A. Weinhold, J. Chem. Phys. 78, 4066-4073, 1983.
- [45] A. E. Reed, R. B. Weinstock, F. A. Weinhold, J. Chem. Phys. 83, 735-746, 1985.
- [46] C. Baker. Metal Science Journal, 5, 1971, 92-100.

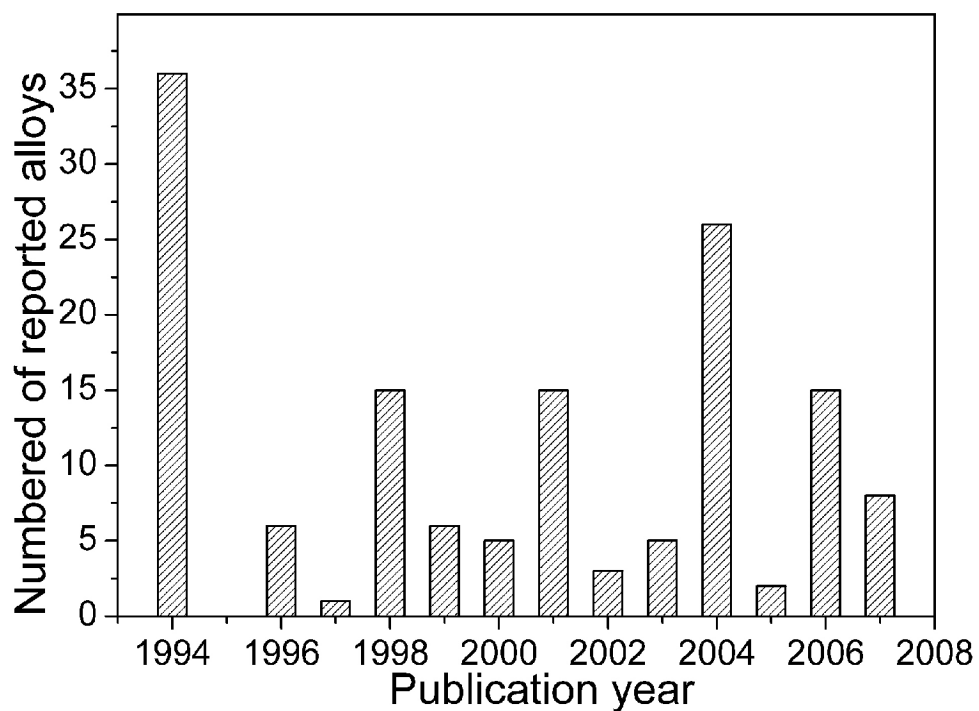
- 1
2
3 [47] H. Sasano, T. Suzuki. In: G. Lutjering, U. Zwicker and W. Bunk, Editors,
4 Proceedings of the 5th International Conference on Titanium DGM, Weinheim (1985), p.
5 1667.
6
7
8
9
10 [48] R. Boyer, G. Welsch, E.W. Collings. Materials Properties Handbook: Titanium
11 Alloys. ASM International, Materials Park, OH, USA, 1994.
12
13 [49] T. Grosdidier, M.J. Philippe. Mater. Sci. Eng. A., 291, (2000), p.218.
14
15 [50] C. Lei, M. Wu, L. McD. Schetky, C. Burstone. In: SMST-97- Proceedings of the
16 Second International Conference on Shape Memory and Superelastic Technologies, (Eds.
17 A. Pelton, et al.), Pacific Grove, California, USA, 1997, p.503.
18
19
20
21
22 [51] Y.Okasaki, S. Rao, Y. Ito, T. Tateisi. Biomaterials, 19, 1998, 1197-1215.
23
24 [52] J. Black, G. Hasting. Handbook of Biomaterials Properties. Chapman and Hall,
25 editors. 1998.
26
27 [53] W.F. Ho, C.P. Ju, J.H. Chern Lin. Biomaterials, 20, 1999, 2115-2122.
28
29 [54] X. Tang, T. Ahmed, H.J. Rack. J. Mater. Sci., 35, 2000, 1805-1811.
30
31 [55] K. Nitta, S. Watanabe, N. Masahashi, H. Hosada, S.Hanawa. In: M. Niinomi, T.
32 Okabe, E.M. Taleff, D.R. Lesuer, H.F. Lippard, editors, Structural Biomaterials for the
33 21st Century, TMS, 2001, 25-34.
34
35 [56] P. Olier, L. Chandrasekaran. Materiaux (France), 2002, 349-354.
36
37 [57] E. Takahashi, S. Watanabe, S. Hanada. In: The International Conference on Shape
38 Memory and Superelastic Technologies, USA, 2003, p.91.
39
40 [58] H.Y. Kim, Y. Ohmatsu, J.I. Kim, H. Hosoda, S. Miyazaki. Mater. Trans. 45,
41 2004, 1090-1095.
42
43 [59] M. Ikeda, S-Y. Komatsu, Y. Nakamura. Mater. Trans. 43, 2002, 2984-2990.
44
45
46
47
48
49
50
51
52
53
54
55
56
57
58
59
60

- 1
2
3
4 [60] T. Ozaki, H. Matsumoto, S. Watanabe, S. Hanada. *Mater. Trans.*, 45, 2004, 2776-
5
6 2779.
7
8 [61] R. Banerjee, S. Nag, J. Stechschulte, H.L. Fraser. *Biomaterials*, 25, 2004, 3413-
9
10 3419.
11
12 [62] Y.J. Hon, J.Y. Wang, R.R. Jeng, C.H. Yeh, Y.N. Pan. *Journal of Taiwan Foundry*
13
14 *Society*, 30, 2004, 33-40.
15
16 [63] N. Sakaguchi, M. Niimori, T. Akahori. *Mater. Trans.*, 45, 2004, 1113-1119.
17
18 [64] T. Maeshima, M. Nishida. *Mater. Trans.* 45, (2004), 1096-1100.
19
20 [65] J.I. Kim, H.Y. Kim, T. Inamura, H. Hosoda, S. Miyazaki. *Mater. Sci. Eng. A.*,
21
22 403, 2005, 334-339.
23
24 [66] C.W. Gong, Y. N. Wang, D.Z. Yang, *Mater. Chem. Phys.*, 96, 2006, 183-187.
25
26 [67] D.H. Ping, C.Y. Cui, F.X. Yin, Y. Yamabe-Mitarai. *Scripta Mater.*, 54, 2006,
27
28 1305-1310.
29
30 [68] Y. Horiuchi, K. Nakayama, T. Inamura, H.Y. Kim, K. Wakashima, S. Miyazaki,
31
32 H. Hosoda. *Mater. Trans.* 48, (2007), 414-421.
33
34 [69] H.Y. Kim, N. Oshika, J.I. Kim, T. Inamura, H. Hosoda, S. Miyazaki. *Mater.*
35
36 *Trans.* 48, (2007), 400-406.
37
38 [70] Y.L. Hao, M. Niinomi, K. Fukunaga, Y.L. Zhou, R. Yang, A. Suzuki. *Metall.*
39
40 *Mater. Trans.*, 33, 2002, 3137-3144.
41
42 [71] Y.G. Gogotsi, V. Domnich. *J. Mater. Res.*, 15, 2000, 871-879.
43
44 [72] C.P. Frick, T.W. Lang, K. Spark, K. Gall. *Acta. Mater.*, 54, 2006, 2223-2234
45
46 [73] Y. Horiuchi, K. Nakayama, T. Inamura, H.Y. Kim, K. Wakashima, S. Miyazaki,
47
48 H. Hosoda. *Mater. Trans.* 48, (2007), 414-421.
49
50
51
52
53
54
55
56
57
58
59
60

- 1
2
3 [74] Y. Horiuchi, T. Inamura, H.Y. Kim, K. Wakashima, S. Miyazaki, H. Hosoda.
4
5 Mater. Trans. 48, (2007), 407-413.
6
7
8 [75] W.C. Oliver, G.M. Pharr. J. Mater. Res., 19, no.1, 2004, 3-20.
9
10

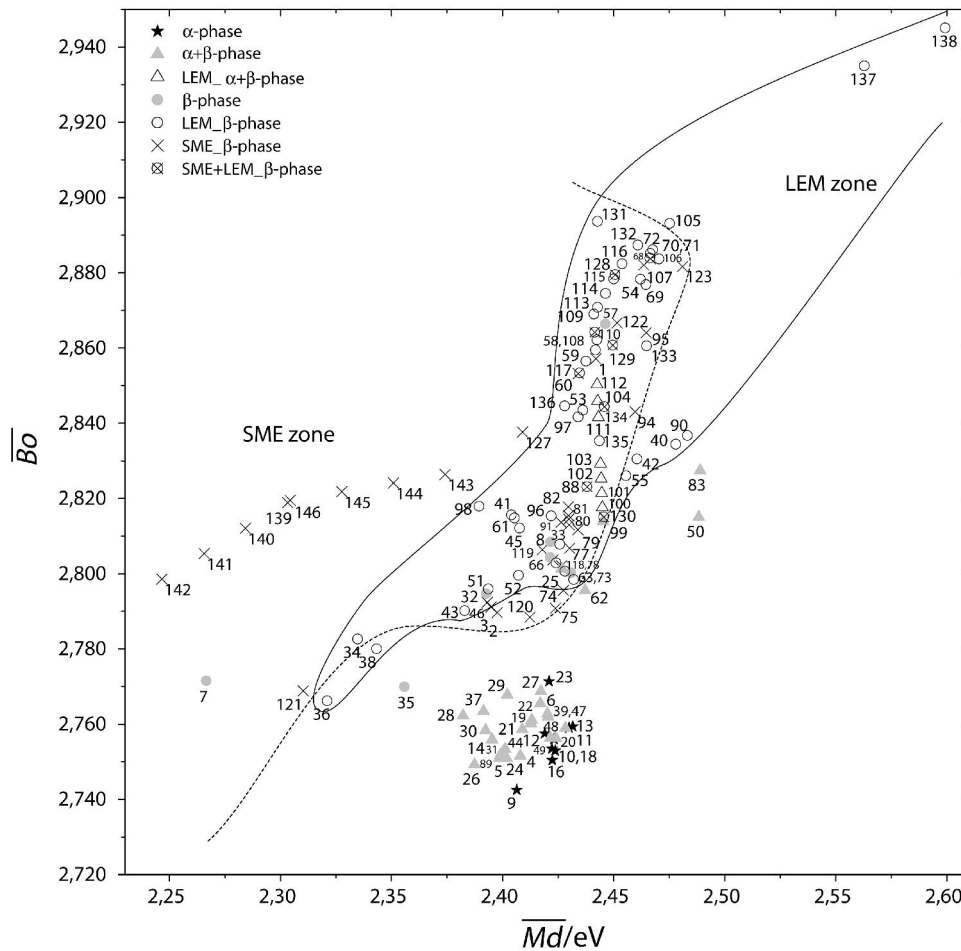
11 12 13 **Figure Legends** 14

- 15
16 Figure 1. Number of publications per year about low elastic modulus and shape
17 memory alloys, from 1994 to 2008.
18
19 Figure 2. Alloy chart based on the *OE* and *BO* parameters proposed in the present
20 work (see table 1). The mapped alloys are those listed in table 2. The
21 solid line encloses the alloys with LEM, and the dashed line those with
22 SME.
23
24 Figure 3. Alloy chart based on the *Md* and *Bo* parameters proposed by Morinaga
25 and coworkers (see table 1). The mapped alloys are those listed in table
26 2, except for those containing O, Bi or Ga. The solid line encloses the
27 alloys with LEM, and the dashed line those with SME.
28
29 Figure 4. Optical micrographs show β -prior grains (a), β -prior grains and α'' -plates
30 within them (b) and mainly α'' -phase (c) in the alloys 131, 129 and 134,
31 respectively.
32
33 Figure 5. X-ray diffraction patterns of the designed and fabricated alloys.
34
35 Figure 6. DSC plots of the alloys 131 and 134 after heat treatment. The alloy
36 number 134 presents an *Ms* temperature of 45°C and the alloy 131 did
37 not evidenced thermoelastic martensite transformation.
38
39 Figure 7. Nanoindentation load-displacement behaviour of the alloys 128, 130 and
40 131 obtained under cyclic increasing-load-control conditions. The rows
41 mark the hysteresis between loading and unloading portions.
42
43
44
45
46
47
48
49
50
51
52
53
54
55
56
57
58
59
60



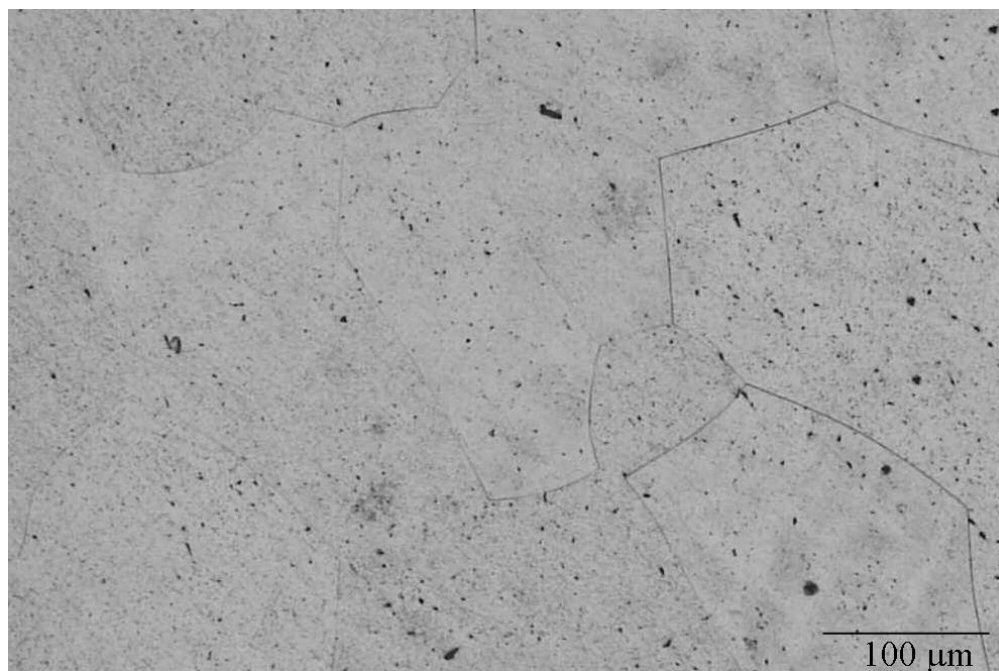
Number of publications per year about low elastic modulus and shape memory alloys, from 1994 to 2007.

83x60mm (600 x 600 DPI)



Alloy chart based on the Md and Bo parameters proposed by Morinaga and coworkers (see table 1). The mapped alloys are those listed in table 2, except for those containing O, Bi or Ga. The solid line encloses the alloys with LEM, and the dashed line those with SME.
160x161mm (600 x 600 DPI)

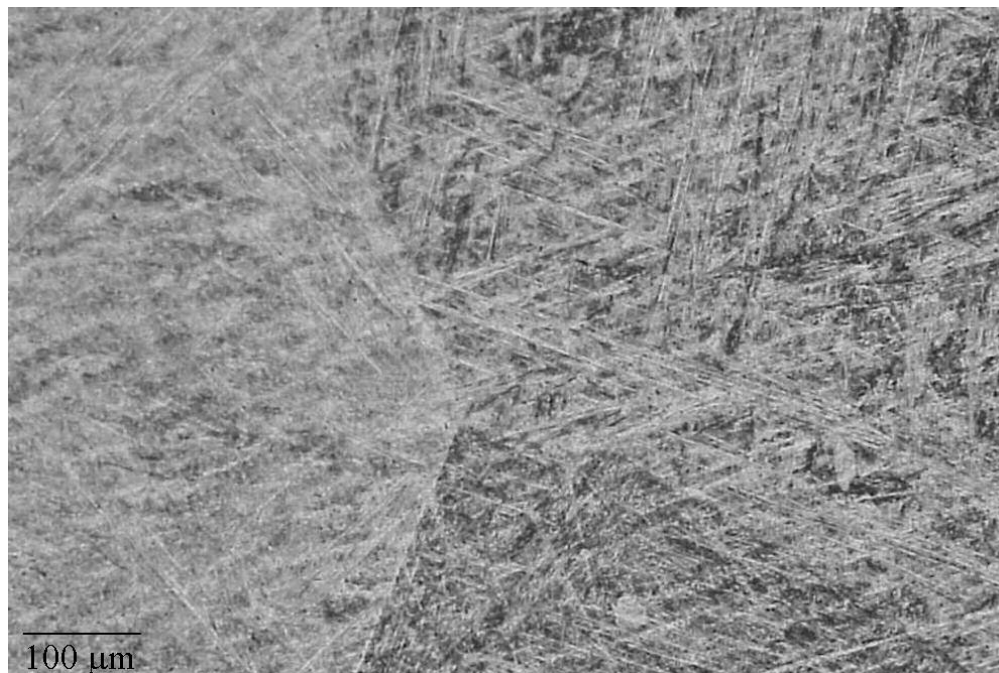




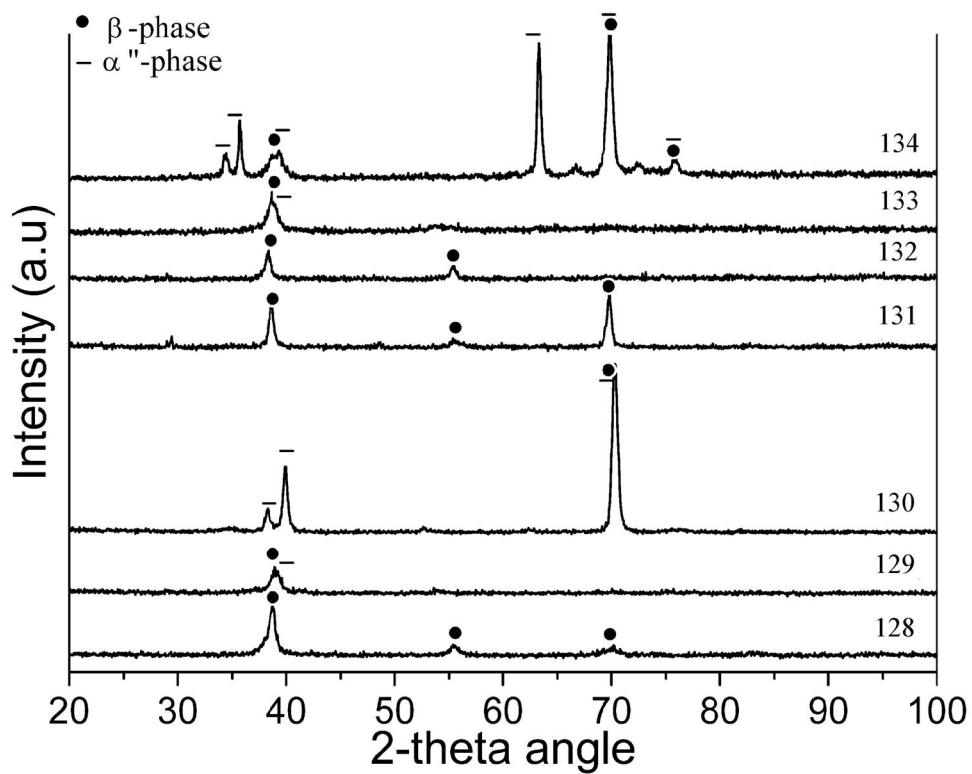
Optical micrographs show β -prior grains (a), β -prior grains and α -plates within them (b) and mainly α -phase (c) in the alloys 131, 129 and 134, respectively.
83x55mm (300 x 300 DPI)



Optical micrographs show β -prior grains (a), β -prior grains and α -plates within them (b) and mainly α -phase (c) in the alloys 131, 129 and 134, respectively.
83x56mm (300 x 300 DPI)



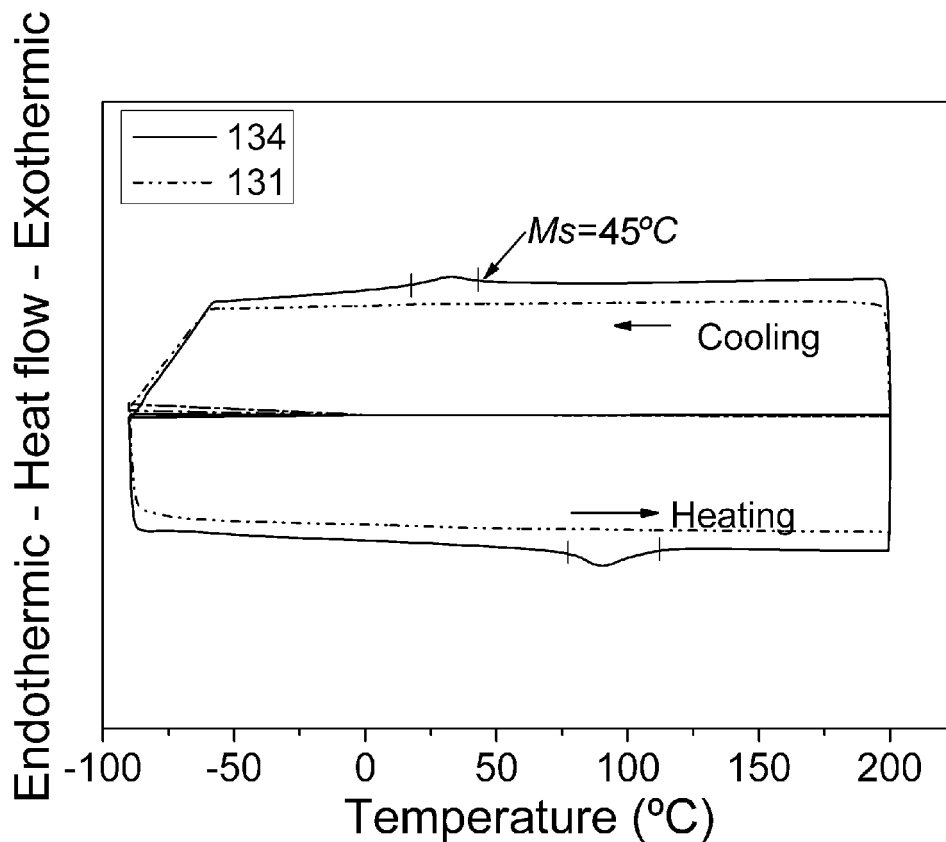
Optical micrographs show β -prior grains (a), β -prior grains and α -plates within them (b) and mainly α -phase (c) in the alloys 131, 129 and 134, respectively.
83x56mm (300 x 300 DPI)



X-ray diffraction patterns of the designed and fabricated alloys.

66x52mm (600 x 600 DPI)

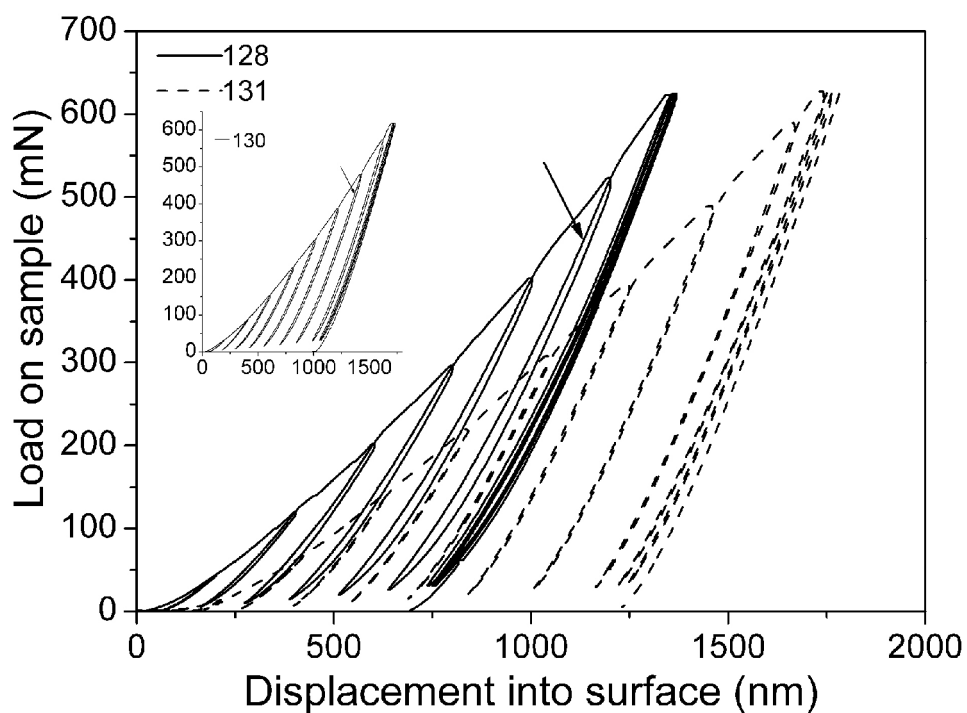
1
2
3
4
5
6
7
8
9
10
11
12
13
14
15
16
17
18
19
20
21
22
23
24
25
26
27
28
29
30
31
32
33
34
35
36
37
38
39
40
41
42
43
44
45
46
47
48
49
50
51
52
53
54
55
56
57
58
59
60



DSC plots of the alloys 131 and 134 after heat treatment. The alloy number 134 presents an Ms temperature of 45°C and the alloy 131 did not evidenced thermoelastic martensite transformation.

83x72mm (600 x 600 DPI)

Only



Nanoindentation load-displacement behaviour of the alloys 128, 130 and 131 obtained under cyclic increasing-load-control conditions. The rows mark the hysteresis between loading and unloading portions.

83x60mm (600 x 600 DPI)

Table 1. Quantum parameters calculated in the present work and those proposed by M. Morinaga and co-workers [24,26].

| Element | Values obtained in the present work | | Values obtained by Morinaga and co-workers | |
|---------|-------------------------------------|-------------------|--|--------------|
| | <i>BO</i> | <i>OE/hartree</i> | <i>Bo</i> | <i>Md/eV</i> |
| O | 0.0864 | 0.19248 | - | - |
| Al | 0.5277 | 0.16041 | 2.426 | 2.200 |
| Si | 0.5163 | 0.14593 | 2.561 | 2.200 |
| Ti | 0.6041 | 0.15454 | 2.790 | 2.447 |
| V | 0.6498 | 0.15438 | 2.805 | 1.872 |
| Cr | 0.6299 | 0.15445 | 2.779 | 1.478 |
| Mn | 0.5710 | 0.15305 | 2.723 | 1.194 |
| Fe | 0.4482 | 0.15270 | 2.651 | 0.969 |
| Co | 0.3856 | 0.15244 | 2.529 | 0.807 |
| Ni | 0.3368 | 0.15137 | 2.412 | 0.724 |
| Cu | 0.3083 | 0.14949 | 2.114 | 0.567 |
| Ga | 0.5227 | 0.11182 | - | - |
| Ge | 0.5009 | 0.15247 | - | - |
| Zr | 0.6827 | 0.17708 | 3.086 | 2.934 |
| Nb | 0.6207 | 0.14741 | 3.099 | 2.424 |
| Mo | 0.5768 | 0.14729 | 3.063 | 1.961 |
| Pd | 0.3601 | 0.14653 | 2.208 | 0.347 |
| Ag | 0.3288 | 0.14386 | 2.094 | 0.196 |
| Sn | 0.5182 | 0.14086 | 2.283 | 2.100 |
| Hf | 0.6698 | 0.14857 | 3.110 | 2.975 |
| Ta | 0.6229 | 0.14723 | 3.144 | 2.531 |
| Pt | 0.3685 | 0.14787 | 2.252 | 0.146 |
| Au | 0.2916 | 0.13708 | 1.953 | 0.258 |
| Bi | 0.5234 | 0.14607 | - | - |

Table 2. Shape memory and low elastic modulus Ti-alloys reported in literature from 1970 to 2007. ST: solution treated; WQ: water quenching; An: annealing; Ag: aging; AC: air cooling; OQ: oil quenching; CW: cold working, Sr: sheet rolled, Hr: Hot rolled, Cd: cold drawing. Ms: martensitic start temperature; Tr: room temperature; SE: superelasticity; SME: shape memory effect.

| N° | Year | Ref | Chemical composition (wt.%) | Conditions | Phase | E (GPa) | Ms (°C) |
|----|------|-----|--------------------------------------|-------------|-------------------------|---------|-------------|
| 1 | 1970 | 46 | Ti-35Nb | WQ,CW,An,WQ | $\beta+\alpha''+\omega$ | | $M_s < T_r$ |
| 2 | 1985 | 4 | Ti-14Mo-3Al | ST, WQ | $\beta+\alpha''$ | | SME |
| 3 | 1985 | 47 | Ti-15Mo-3Al | ST, WQ | $\beta+\alpha''$ | | SME |
| 4 | 1994 | 48 | Ti-7Al-4Mo | ST,An | $\alpha+\beta$ | 111 | |
| b | 1994 | 48 | Ti-7Al-4Mo | ST,Ag | $\alpha+\beta$ | 116 | |
| 5 | 1994 | 48 | Ti-5Al-5Sn-2Zr-2Mo-2Cr-0.25Si | ST,An | $\alpha+\beta$ | 114 | |
| 6 | 1994 | 48 | Ti-4Al-2Sn-4Mo | ST,Ag | $\alpha+\beta$ | 115 | |
| 7 | 1994 | 48 | Ti-13V-11Cr-3Al | ST | β | 101 | |
| b | 1994 | 48 | Ti-13V-11Cr-3Al | ST,Ag | β | 110 | |
| 8 | 1994 | 48 | Ti-4Sn-6Zr-11.5Mo-0.35Fe | ST,An | β | 103 | |
| 9 | 1994 | 48 | Ti-8Al-1Mo-1V | Duplex An | α | 120 | |
| 10 | 1994 | 48 | Ti-5Al-2.5Sn | ST,An | α | 110-125 | |
| 11 | 1994 | 48 | Ti-11Sn-5Zr-2.25Al-1Mo-0.25Si | Duplex An | α | 114 | |
| 12 | 1994 | 48 | Ti-6Al-2Nb-1Ta-1Mo | Sr | α | 114 | |
| 13 | 1994 | 48 | Ti-6Al-5Zr-0.5Mo-0.25Si IMI 685 | ST,OQ,Ag | α | 125 | |
| 14 | 1994 | 48 | Ti-5Al-2.5Fe | Sr | $\alpha+\beta$ | 110 | |
| 15 | 1994 | 48 | Ti-6Al-2Sn-1.5Zr-1Mo-0.35Bi-0.1Si | ST,An | α | | |
| 16 | 1994 | 48 | Ti-5.5Al-3.5Sn-3Zr-1Nb-0.3Mo-0.3Si | ST,An | α | | |
| 17 | 1994 | 48 | Ti-5.8Al-4Sn-3.5Zr-0.7Nb-0.5Mo-0.3Si | ST,An | α | | |
| 18 | 1994 | 48 | Ti-6Al-2Sn-4Zr-2Mo-0.08Si | ST,An | α | 114 | |
| 19 | 1994 | 48 | Ti-4Al-4Sn-4Mo-0.25Si | ST,An | $\alpha+\beta$ | | |
| 20 | 1994 | 48 | Ti-2Al-11Sn-4Zr-1Mo-0.25Si | ST,An | $\alpha+\beta$ | | |
| 21 | 1994 | 48 | Ti-6Al-5Zr-4Mo-1Cu-0.2Si | ST,An | $\alpha+\beta$ | | |
| 22 | 1994 | 48 | Ti-6Al-2Sn-4Zr-6Mo | ST,An | $\alpha+\beta$ | 114 | |
| 23 | 1994 | 48 | Ti-3Al-2.5V | St,An | α | 105 | |
| 24 | 1994 | 48 | Ti-6Al-1.65Fe | An | $\alpha+\beta$ | 127 | |
| 25 | 1994 | 48 | Ti-8Mo | ST,An | $\alpha+\beta$ | 113 | |
| 26 | 1994 | 48 | Ti-6Al-6V-2Sn | ST,An | $\alpha+\beta$ | 110 | |
| 27 | 1994 | 48 | Ti-4Al-3Mo-1V | ST,Ag | $\alpha+\beta$ | 117 | |
| 28 | 1994 | 48 | Ti-4.5Al-3V-2Mo-2Fe | An | $\alpha+\beta$ | 110 | |
| 29 | 1994 | 48 | Ti-4.5Al-5Mo-1.5Cr | An | $\alpha+\beta$ | 114 | |
| 30 | 1994 | 48 | Ti-5Al-1.5Fe-1.4Cr-1.2Mo | An | $\alpha+\beta$ | 114 | |
| 31 | 1994 | 48 | Ti-6Al-2Sn-2Zr-2Mo-2Cr-0.25Si | An | $\alpha+\beta$ | 114 | |
| 32 | 1994 | 48 | Ti-15Mo-3Al-2.7Nb-0.25Si | ST, An,Ag | β | 97 | |

| | | | | | | | |
|----|------|----|---------------------------------------|----------|------------------|--------|-----|
| | | | TIMETAL 21S | | | | |
| | | | Ti-15Mo-3Al-2.7Nb-0.25Si | | | | |
| b | 1997 | 6 | TIMETAL 21S | ST,An | β | 74 | |
| 33 | 1994 | 48 | Ti-11.5Mo-6Zr-4.5Sn BETA III | ST,An | β | 68 | |
| b | 1994 | 48 | Ti-11.5Mo-6Zr-4.5Sn BETA III | ST,Ag | β | 102 | |
| 34 | 1994 | 48 | Ti-3Al-8V-6Cr-4Mo-4Zr BETA C | ST,An | β | 80 | |
| 35 | 1994 | 48 | Ti-10V-2Fe-3Al | ST,An | β | 112 | |
| 36 | 1994 | 48 | Ti-15V-3Al-3Cr-3Sn | ST | β | 81 | |
| 37 | 1994 | 48 | Ti- 5Al-2Sn-4Zr-4Mo-2Cr-1Fe | ST,Ag | $\alpha+\beta$ | 122 | |
| b | 2000 | 49 | Ti- 5Al-2Sn-4Zr-4Mo-2Cr-1Fe | ST,WQ | $\beta+\alpha''$ | | SME |
| 38 | 1994 | 48 | Ti-8Mo-8V-2Fe-3Al | ST | β | 70 | |
| 39 | 1994 | 48 | Ti-6Al-7Nb | ST,An,AC | $\alpha+\beta$ | 105 | |
| 40 | 1996 | 5 | Ti-12.5Nb-12.5Zr-0.25Fe | ST,Ag | β | 82 | |
| 41 | 1996 | 5 | Ti-12Mo-6Zr-2Fe (TMZF TM) | ST,WQ | β | 74 | |
| 42 | 1996 | 5 | Ti-16.5Nb-9.5Hf Tiadyne 1610 | ST,Ag | β | 81 | |
| 43 | 1996 | 5 | Ti-15Mo-3Nb Timetal 21SRx | An | β | 83 | |
| 44 | 1996 | 5 | Ti-6Al-4V | ST,An | $\alpha+\beta$ | 110 | |
| 45 | 1996 | 5 | Ti-15Mo | ST,An,WQ | β | 78 | |
| 46 | 1997 | 50 | Ti-11Mo-3Al-2V-4Nb | ST,WQ | $\beta+\alpha''$ | | SME |
| 47 | 1998 | 51 | Ti-6Al-6Nb-1Ta | | $\alpha+\beta$ | | |
| 48 | 1998 | 51 | Ti-6Al-2Nb-1Ta | | $\alpha+\beta$ | | |
| 49 | 1998 | 51 | Ti-15Sn | | $\alpha+\beta$ | | |
| 50 | 1998 | 51 | Ti-15Zr | | $\alpha+\beta$ | | |
| 51 | 1998 | 6 | Ti-15Mo-2.8Nb-3Al | ST,WQ | β | 82 | |
| b | 1998 | 6 | Ti-15Mo-2.8Nb-3Al | ST,Ag | $\alpha+\beta$ | 100 | |
| 52 | 1998 | 6 | Ti-15Mo-5Zr-3Al | ST,WQ | β | 75 | |
| b | 1998 | 6 | Ti-15Mo-5Zr-3Al | ST,Ag | $\alpha+\beta$ | 88-113 | |
| 53 | 1998 | 21 | Ti-16Nb-13Ta-4Mo | ST,WQ | β | 46 | |
| b | 1998 | 21 | Ti-16Nb-13Ta-4Mo | ST,Ag | β | 98 | |
| 54 | 1998 | 21 | Ti-29Nb-13Ta-4.6Zr | ST,CW | β | 50 | |
| b | 1998 | 21 | Ti-29Nb-13Ta-4.6Zr | ST,Ag | β | 80 | |
| c | 2003 | 7 | Ti-29Nb-13Ta-4.6Zr | ST,WQ | β | 63 | SE |
| d | 2003 | 7 | Ti-29Nb-13Ta-4.6Zr | ST,WQ+Ag | β | 97 | |
| e | 2003 | 7 | Ti-29Nb-13Ta-4.6Zr | ST,WQ+CW | β | 62 | SE |
| 55 | 1998 | 52 | Ti-30Ta | Sr | β | 80 | SME |
| b | 1998 | 52 | Ti-30Ta | ST,WQ | β | 63 | SME |
| 56 | 1998 | 48 | Ti-55.1Ni | ST,An | $\beta+\alpha''$ | 68 | SME |
| 57 | 1998 | 21 | Ti-29Nb-13Ta | Ag | β | 105 | |
| 58 | 1998 | 21 | Ti-29Nb-13Ta-2Sn | ST,Ag | β | 48 | |
| 59 | 1998 | 21 | Ti-29Nb-13Ta-4.6Sn | ST,Ag | β | 76 | |
| 60 | 1998 | 21 | Ti-29Nb-13Ta-6Sn | ST,Ag | β | 65 | |
| 61 | 1998 | 6 | Ti-11.5Mo-6Zr-2Fe | ST | β | 74-85 | |
| 62 | 1999 | 53 | Ti-4Mo | Casted | $\alpha+\beta$ | | |

| | | | | | | | |
|-----|------|----|----------------------------|------------|-------------------------|-----|------|
| 63 | 1999 | 53 | Ti-6Mo | Casted | β | 64 | |
| 64 | 1999 | 53 | Ti-7.5Mo | Casted | β | 55 | |
| 65 | 1999 | 53 | Ti-9Mo | Casted | $\beta+\alpha''$ | 75 | |
| 66 | 1999 | 53 | Ti-10Mo | Casted | β | 95 | |
| 67 | 1999 | 12 | Ti-15Sn-4Nb-2Ta-0.2Pd-0.2O | ST,Ag | $\alpha+\beta$ | 100 | |
| 68 | 2000 | 54 | Ti-24Nb-22Ta-4.5Zr | ST,WQ | $\beta+\alpha''+\omega$ | 55 | |
| 69 | 2000 | 54 | Ti-22Nb-22Ta-4Zr | ST,WQ | $\beta+\alpha''+\omega$ | 65 | |
| 70 | 2000 | 54 | Ti-29Nb-12.5Ta-7Zr | ST,WQ | $\beta+\omega$ | 50 | |
| 71 | 2000 | 54 | Ti-35.5Nb-5Ta-7Zr | ST,WQ | $\beta+\omega$ | 56 | |
| 72 | 2000 | 54 | Ti-35.1Nb-5.7Ta-7.2Zr | ST,WQ | $\beta+\omega$ | 48 | |
| 73 | 2001 | 55 | Ti-16.6Nb-8.6Sn | ST,WQ,Ag | β | | |
| 74 | 2001 | 55 | Ti-16.6Nb-10.6Sn | ST,WQ,Ag | β | | SME |
| 75 | 2001 | 55 | Ti-16.6Nb-12.6Sn | ST,WQ,Ag | β | | 66 |
| 76 | 2001 | 55 | Ti-20Nb-6.4Sn | ST,WQ,Ag | β | | -20 |
| 77 | 2001 | 55 | Ti-20Nb-8.6Sn | ST,WQ,Ag | β | | 66 |
| 78 | 2001 | 55 | Ti-20Nb-10.6Sn | ST,WQ | β | | SE |
| 79 | 2001 | 55 | Ti-22.8Nb-8.3Sn | ST,WQ,Ag | β | | SME |
| 80 | 2001 | 55 | Ti-23.5Nb-8.3Sn | ST,WQ | β | | SME |
| 81 | 2001 | 55 | Ti-24Nb-8.3Sn | ST,WQ | β | | SME |
| 82 | 2001 | 55 | Ti-25Nb-8.2Sn | ST,WQ | β | | SME |
| 83 | 2001 | 19 | Ti-15Zr-4Nb-4Ta-0.2Pd | ST,An | $\alpha+\beta+\alpha'$ | 100 | |
| b | 2001 | 19 | Ti-15Zr-4Nb-4Ta-0.2Pd | ST, Ag | $\beta+\alpha'$ | 97 | |
| 84 | 2001 | 17 | Ti-47.75Ni-5.78Cu-5.24Mo | Hr, Cd, ST | β | | -8 |
| 85 | 2001 | 17 | Ti-46.74Ni-5.68Cu-5.58Mo | Hr, Cd, ST | β | | -18 |
| 86 | 2001 | 17 | Ti-44.35Ni-5.45Cu-16.47Mo | Hr, Cd, ST | β | | -103 |
| 87 | 2001 | 17 | Ti-49.34Ni-5.93Cu | Hr, Cd, ST | β | | SME |
| 88 | 2002 | 56 | Ti-24Nb-1.5Al-1Hf | ST,WQ | β | 35 | 20 |
| 89 | 2003 | 7 | Ti-6.42Al-4.19V ELI | ST, WQ | $\alpha+\beta$ | 118 | |
| 90 | 2003 | 7 | Ti-13Nb-13Zr | ST,WQ | β | 64 | |
| b | 2003 | 7 | Ti-13Nb-13Zr | ST,WQ,Ag | β | 81 | |
| c | 2003 | 7 | Ti-13Nb-13Zr | ST,AC | β | 83 | |
| d | 2003 | 7 | Ti-13Nb-13Zr | ST,WQ,CW | β | 44 | |
| 91 | 2003 | 57 | Ti-25Nb-10Sn | ST,WQ | β | | SE |
| 92 | 2003 | 58 | Ti-13Mo-5.3Ga | ST,WQ | β | | SME |
| 93 | 2003 | 58 | Ti-11.2Mo-4.1Ga | ST,WQ | β | | SME |
| 94 | 2002 | 59 | Ti-40Ta | ST,WQ | $\beta+\alpha''$ | | 350 |
| 95 | 2002 | 59 | Ti-50Ta | ST,WQ | $\beta+\alpha''$ | | 400 |
| 96 | 2004 | 60 | Ti-27.87Nb-11.87Sn | ST,WQ | β | 40 | |
| 97 | 2004 | 60 | Ti-32.52Nb-4.75Sn | ST,WQ, CW | β | 43 | |
| 98 | 2004 | 61 | Ti-13Mo-7Zr-3FeTMZF | ST,Ag, AC | β | 89 | |
| 99 | 2004 | 62 | Ti-14Nb | ST,An | $\alpha+\beta$ | 95 | |
| 100 | 2004 | 62 | Ti-16 Nb | ST,An | $\alpha+\beta$ | 88 | |
| 101 | 2004 | 62 | Ti-18 Nb | ST,An | $\alpha+\beta$ | 84 | |
| 102 | 2004 | 62 | Ti-20 Nb | ST,An | $\alpha+\beta$ | 84 | |

| | | | | | | | |
|-----|------|----|---------------------------|----------------|-------------------------|-------|-----|
| 103 | 2004 | 62 | Ti-22 Nb | ST,An | $\alpha+\beta$ | 78 | |
| 104 | 2004 | 62 | Ti-30 Nb | ST, WQ | $\alpha+\beta+\omega$ | 70 | |
| 105 | 2004 | 63 | Ti-34Nb-9Zr-8Ta | ST,Ag | β | 89 | |
| 106 | 2004 | 20 | Ti-35Nb-5Ta-7Zr | ST,WQ | β | | SE |
| 107 | 2004 | 63 | Ti-30Nb-13Ta-5Zr (TNZT30) | ST,AC | β | | SE |
| 108 | 2004 | 62 | Ti-36Nb | ST,WQ | $\beta+\omega$ | 77 | |
| 109 | 2004 | 62 | Ti-40Nb | ST,WQ | $\beta+\omega$ | 55 | |
| 110 | 2004 | 62 | Ti- 38Nb | ST,WQ | $\beta+\omega$ | 66 | SME |
| 111 | 2004 | 62 | Ti-28Nb | ST,WQ | $\alpha+\beta$ | 82 | |
| 112 | 2004 | 62 | Ti-32Nb | ST,WQ | $\alpha+\beta+\omega$ | 85 | |
| 113 | 2004 | 20 | Ti-40Nb-1Hf | ST, An, FC | $\beta+\omega$ | 65 | |
| 114 | 2004 | 20 | Ti-40Nb-3Hf | ST, An, FC | $\beta+\omega$ | 62 | |
| 115 | 2004 | 20 | Ti-40Nb-5Hf | ST, An, FC | $\beta+\omega$ | 67 | |
| 116 | 2004 | 20 | Ti-40Nb-7Hf | ST, An, FC | $\beta+\omega$ | 63 | |
| 117 | 2004 | 16 | Ti-38.41Nb-1.4Al | ST,WQ,ST,WQ | $\beta+\omega$ | | -72 |
| 118 | 2004 | 64 | Ti-9,54Mo | ST,HW,CW,ST,WQ | $\beta+\alpha''$ | | SME |
| 119 | 2004 | 64 | Ti-11,34Mo | ST,HW,CW,ST,WQ | $\beta+\alpha''$ | | SME |
| 120 | 2004 | 64 | Ti-9,15Mo-6,80Sn | ST,HW,CW,ST,WQ | β | | SME |
| 121 | 2004 | 64 | Ti-9Mo-10.12Ag | ST,HW,CW,ST,WQ | $\beta+\alpha''$ | | SME |
| 122 | 2005 | 65 | Ti-36Nb-3.1Zr | CW, ST, WQ | β | | 37 |
| 123 | 2005 | 65 | Ti-33.4Nb-12Zr | CW, ST, WQ | β | | -60 |
| 124 | 2006 | 66 | Ti-51.2Ni-9.5Ta | ST,An,WQ | β | | 58 |
| 125 | 2006 | 66 | Ti-49Ni-15.1Ta | ST,An,WQ | β | | 44 |
| 126 | 2006 | 66 | Ti-46.2Ni-14.5Ta | ST,An,WQ | β | | 55 |
| 127 | 2006 | 67 | Ti-30Nb-3Pd | ST,WQ, An,WQ | $\beta+\omega+\alpha''$ | | SME |
| 128 | 2006 | | Ti-24.73Nb-24.70Ta | ST,WQ | β | 75 | |
| 129 | 2006 | | Ti-21.40Nb-20.13Ta | ST,WQ | $\beta+\alpha''$ | 78 | |
| 130 | 2006 | | Ti-13.7Nb-1.4Ta | ST,WQ | $\beta+\alpha''$ | 72 | 125 |
| 131 | 2006 | | Ti-48.50Nb-1Zr | ST,WQ | β | 79 | |
| 132 | 2006 | | Ti-41.20Nb-6.10Zr | ST,WQ | β | 67 | |
| 133 | 2006 | | Ti-29.50Nb-7.13Zr | ST,WQ | $\beta+\alpha''$ | 78 | |
| 134 | 2006 | | Ti-19.1Nb-8.8Zr | ST,WQ | $\beta+\alpha''$ | 74 | 45 |
| 135 | 2006 | 27 | Ti-25Nb | ST,WQ | β | 60-70 | |
| 136 | 2006 | 27 | Ti-30Nb-1Fe | ST,WQ | β | 60-70 | |
| 137 | 2006 | 27 | Ti-50Ta-20Zr | ST,WQ | β | 60-70 | |
| 138 | 2006 | 27 | Ti-34.78Zr-11.81Nb-23Ta | ST,WQ | β | 44 | |
| 139 | 2007 | 68 | Ti-30,30Mo-3,34Cu | ST,WQ,CW,ST,WQ | $\beta+\alpha''$ | | SME |
| 140 | 2007 | 68 | Ti-30,22Mo-4,45Cu | ST,WQ,CW,ST,WQ | β | | SE |
| 141 | 2007 | 68 | Ti-30,13Mo-5,54Cu | ST,WQ,CW,ST,WQ | β | | SE |
| 142 | 2007 | 68 | Ti-30,05Mo-6,64Cu | ST,WQ,CW,ST,WQ | β | | SE |
| 143 | 2007 | 69 | Ti-26,35Nb-9,76Pt | ST,CW,An,WQ | α'' | | SME |
| 144 | 2007 | 69 | Ti-27,03Nb-12,61Pt | ST,CW,An,WQ | $\beta+\alpha''$ | | SE |
| 145 | 2007 | 69 | Ti-27,67Nb-15,29Pt | ST,CW,An,WQ | $\beta+\alpha''$ | | SE |
| 146 | 2007 | 69 | Ti-28,28Nb-17,81Pt | ST,CW,An,WQ | $\beta+\alpha''$ | | SE |

1
2
3
4
5
6
7
8
9
10
11
12
13
14
15
16
17
18
19
20
21
22
23
24
25
26
27
28
29
30
31
32
33
34
35
36
37
38
39
40
41
42
43
44
45
46
47
48
49
50
51
52
53
54
55
56
57
58
59
60

For Peer Review Only

Table 3. Chemical composition (wt.%), β -transus temperature ($^{\circ}\text{C}$) [48], Mo. equivalence (%) [48], microstructure, M_s temperature ($^{\circ}\text{C}$) or thermoelastic phase transformation detected by cyclic nanoindentation (TPT), and elastic modulus values (GPa) for each alloy fabricated in our laboratory.

| Chemical composition | Nr. alloy | β transus temperature | Mo.eq. | Microstructure | M_s temperature | E, 5%error |
|----------------------|-----------|-----------------------------|--------|--------------------------|-------------------|------------|
| Ti-24.73Nb-24.70Ta | 128 | 649 | 12,4 | β | TPT | 75 |
| Ti-21.40Nb-20.13Ta | 129 | 683 | 10,4 | β +some α'' | TPT | 78 |
| Ti-13.7Nb-1.4Ta | 130 | 780 | 4,1 | mainly α'' | 125 TPT | 72 |
| Ti-48.50Nb-1Zr | 131 | 532 | 13,6 | β | - | 79 |
| Ti-41.20Nb-6.10Zr | 132 | 584 | 11,6 | β | - | 67 |
| Ti-29.50Nb-7.13Zr | 133 | 669 | 8,3 | β +some α'' | - | 78 |
| Ti-19.1Nb-8.10Zr | 134 | 713 | 6,6 | mainly α'' | 45 TPT | 74 |